Acta Crystallographica Section F
Structural Biology and Crystallization Communications
ISSN 1744-3091

Towards structural studies of the old yellow enzyme homologue SYE4 from *Shewanella oneidensis* and its complexes at atomic resolution

Jonathan Elegheert,[a] Debbie van den Hemel,[a]‡ Ina Dix,[b] Jan Stout,[a] Jozef Van Beeumen,[a] Ann Brigé[a]§ and Savvas N. Savvides[a]*

[a]Department of Biochemistry and Microbiology, Laboratory for Protein Biochemistry and Biomolecular Engineering (L-ProBE), Ghent University, K. L. Ledeganckstraat 35, 9000 Ghent, Belgium, and [b]Bruker AXS GmbH, Östliche Rheinbrückenstrasse 49, 76187 Karlsruhe, Germany

‡ Current address: Microflor, Lichtelaerestraat 87, 9080 Lochristi, Belgium.
§ Current address: Ablynx NV, Technologiepark 4, 9052 Ghent/Zwijnaarde, Belgium.

Correspondence e-mail: savvas.savvides@ugent.be

Received 19 October 2009
Accepted 23 November 2009

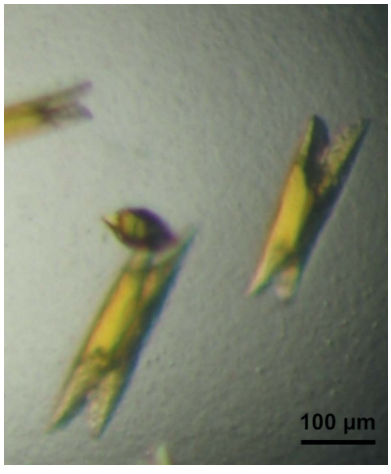

Shewanella oneidensis is an environmentally versatile Gram-negative γ-proteobacterium that is endowed with an unusually large proteome of redox proteins. Of the four old yellow enzyme (OYE) homologues found in *S. oneidensis*, SYE4 is the homologue most implicated in resistance to oxidative stress. SYE4 was recombinantly expressed in *Escherichia coli*, purified and crystallized using the hanging-drop vapour-diffusion method. The crystals belonged to the orthorhombic space group $P2_12_12_1$ and were moderately pseudo-merohedrally twinned, emulating a $P422$ metric symmetry. The native crystals of SYE4 were of exceptional diffraction quality and provided complete data to 1.10 Å resolution using synchrotron radiation, while crystals of the reduced enzyme and of the enzyme in complex with a wide range of ligands typically led to high-quality complete data sets to 1.30–1.60 Å resolution, thus providing a rare opportunity to dissect the structure–function relationships of a good-sized enzyme (40 kDa) at true atomic resolution. Here, the attainment of a number of experimental milestones in the crystallographic studies of SYE4 and its complexes are reported, including isolation of the elusive hydride–Meisenheimer complex.

1. Introduction

Old yellow enzyme (OYE) was discovered in the 1930s and over the years it has served as a model system for study of the requirement of a cofactor in catalysis by enzymes (Massey, 2000). OYE has since been identified in yeasts (Matthews & Massey, 1969), plants (Schaller & Weiler, 1997) and bacteria (French *et al.*, 1996; Blehert *et al.*, 1999; French & Bruce, 1995) but not in animals. OYE-family enzymes have been extensively studied over the years both structurally and biochemically and a number of well studied members have emerged, such as the bacterial pentaerythritol tetranitrate reductase (PETNR; French *et al.*, 1996), morphinone reductase (MorB; French & Bruce, 1994) and YqjM (Fitzpatrick *et al.*, 2003), the plant oxophytodienoic acid reductases *Le*OPR (Strassner *et al.*, 1999) and *At*OPR (Biesgen & Weiler, 1999), several yeast OYEs (Williams & Bruce, 2002) and an enzyme involved in prostaglandin synthesis in *Trypanosoma cruzi* (Kubata *et al.*, 2002). A unifying theme in the functionality of OYE-family enzymes is that they employ a ping-pong reaction mechanism consisting of an oxidative and a reductive half-reaction using NAD(P)H to reduce simple and complex unsaturated aldehydes and ketones, nitro-esters and nitro-aromatic substrates (Williams & Bruce, 2002). Furthermore, OYEs can form long-wavelength charge-transfer interactions with phenolic compounds, which typically bind in the active site *via* stacking interactions with the FMN cofactor and hydrogen bonding of the phenolate hydroxyl to a strictly conserved histidine/asparagine or histidine/histidine pair (Abramovitz & Massey, 1976). In addition, OYEs have been shown to bind to explosive chemicals such as trinitrotoluene (TNT) and picric acid (Khan *et al.*, 2004), thus opening avenues for the usage of OYEs in bioremediation processes (Williams *et al.*, 2004; French *et al.*, 1999; Hannink *et al.*, 2001; Khan *et al.*, 2004). Despite such a rich track record in the structural enzymology of OYE enzymes, there is a stark

Table 1
X-ray data-collection statistics.

Values in parentheses are for the highest resolution shell. HBA, *para*-hydroxybenzaldehyde; MPH, *para*-methoxyphenol; PMP, *para*-methylphenol; TNP, trinitrophenol; RED, reduced; MSH, hydride–Meisenheimer complex.

	Native SYE4	HBA–SYE4	MPH–SYE4	PMP–SYE4	TNP–SYE4	RED–SYE4	MSH–SYE4
Source	SLS X06SA	DESY/EMBL X13	DESY/EMBL X11	DESY/EMBL X11	DESY/EMBL X11	DESY/EMBL X11	DESY/EMBL X11
Detector	Pilatus-6M	MAR 165	MAR 165	MAR 555	MAR 555	MAR 555	MAR 555
Temperature (K)	100	100	100	100	100	100	100
Wavelength (Å)	0.8500	0.8076	0.8148	0.8148	0.8148	0.8148	0.8148
Frame oscillation† (°)	0.250	0.350/0.750	0.500/1.000	0.500	0.500	0.500	0.500
Data-processing software	*XDS*/*XSCALE*	*XDS*/*XSCALE*	*XDS*/*XSCALE*	*XDS*/*XSCALE*	*XDS*/*XSCALE*	*XDS*/*XSCALE*	*XDS*/*XSCALE*
Nominal resolution range (Å)	50.00–1.10	20.00–1.30	20.00–1.50	25.00–1.65	25.00–1.60	25.00–1.45	25.00–1.55
Space group	$P2_12_12_1$	$P2_12_12_1$	$P2_12_12_1$	$P2_12_12_1$	$P2_12_12_1$	$P2_12_12_1$	$P2_12_12_1$
PM twinning‡	Y	Y	Y	Y	Y	Y	N
Unit-cell parameters (Å)							
a	52.23	52.09	52.18	52.26	52.18	52.22	50.43
b	54.81	54.66	54.83	54.79	54.77	54.78	54.47
c	103.55	103.75	103.48	103.67	103.50	103.23	105.27
V_M (Å^3 Da^{-1})	1.90	1.89	1.89	1.90	1.89	1.89	1.85
Apparent mosaicity (°)	0.193	0.085	0.168	0.195	0.235	0.230	0.207
Unique reflections	120389	71571	47629	42707	39489	52643	42455
Multiplicity	4.5	5.3	5.2	4.5	6.9	7.2	5.4
Completeness (%)	99.4 (99.8)	97.3 (95.5)	98.5 (98.9)	97.1 (95.4)	98.9 (96.8)	98.8 (98.2)	99.3 (95.9)
R_{meas}§ (%)	4.6 (34.2)	11.8 (48.8)	8.0 (43.4)	7.0 (54.0)	7.1 (49.4)	6.3 (58.5)	8.8 (60.8)
Average $I/\sigma(I)$	18.3 (4.9)	9.7 (3.8)	18.4 (3.6)	21.8 (2.7)	24.6 (3.8)	29.1 (4.1)	19.9 (3.0)

† When more than two values are given, the first refers to the high-resolution pass and the second to the low-resolution pass; the latter was required owing to detector overloading. ‡ The twin operator is *k*, *h*, −*l*; this transforms the orthorhombic crystal symmetry to the *P*422 tetragonal lattice symmetry. § $R_{meas} = \sum_{hkl}[N/(N-1)]^{1/2}\sum_i |I_i(hkl) - \langle I(hkl)\rangle|/\sum_{hkl}\sum_i I_i(hkl)$, where N is the multiplicity, $I_i(hkl)$ is the intensity of the ith measurement of reflection hkl and $\langle I(hkl)\rangle$ is the average value over multiple measurements. R_{meas} values are from diffraction data untreated for twinning.

lack of knowledge of the physiological role and substrate(s) of such enzymes. Indeed, these issues have been settled for only one member of the OYE family: the plant enzyme 12-oxophytodienoate reductase 3 (OPR3), which catalyzes one step in the biosynthesis of the plant hormone jasmonic acid (JA; Schaller *et al.*, 2000).

Probing the *Shewanella oneidensis* MR-1 genome for OYE-family members led to the identification of four homologues (NP718044, NP718043, NP719682 and NP718946), which were termed SYE1–4 (Brigé *et al.*, 2006). *In vivo* analysis showed that only SYE4 is induced under conditions of elevated oxidative stress, while *in vitro* characterization demonstrated striking differences in ligand binding, catalytic efficiency and substrate specificity between SYE4 and the other SYE homologues (Brigé *et al.*, 2006). Here, we report preliminary crystallographic studies of liganded and unliganded SYE4 at atomic resolution, with special reference to the isolation in the crystal of a hitherto elusive hydride–Meisenheimer complex, the product of the enzymatic two-electron reduction (inactivation) of the explosive trinitrophenol (TNP) by an OYE.

2. Materials and methods

2.1. Cloning, protein expression and purification

The *sye4* gene was cloned in the second multiple cloning site of the pACYC-Duet-1 vector (Novagen), between the *Nde*I and *Xho*I restriction sites, generating pACYC-SYE4. This cloning strategy puts *sye4* out of frame with the His tag. The pACYC-SYE4 vector was transformed into *Escherichia coli* BL21 (DE3) cells. The cultures were grown at 291 K under constant shaking and SYE4 expression was induced at an $A_{600\,nm}$ of 0.6 using 0.5 m*M* isopropyl β-D-1-galactopyranoside (IPTG). After 4 h further growth, the cells were harvested by centrifugation and resuspended in 10 ml 50 m*M* Tris pH 8.0 per litre of culture. The resuspended cells were lysed by sonication and the soluble fraction was clarified by centrifugation (25 000*g*, 1 h). SYE4 was purified in three steps. Lysate containing SYE4 was manually loaded onto a Q-Sepharose FF column (10 ml bed volume) equilibrated with 50 m*M* Tris pH 8.0. The column was washed with 50 m*M* Tris pH 8.0, 50 m*M* NaCl and SYE4 was eluted with 50 m*M* Tris pH 8.0, 300 m*M* NaCl. The eluate was dialyzed to remove the salt and was loaded onto a Source 30Q column (10 ml bed volume) equilibrated with 50 m*M* Tris pH 8.0. SYE4 eluted at 200 m*M* NaCl. The pooled fractions were loaded onto a Superdex 75 column (120 ml bed volume) equilibrated with 50 m*M* Tris pH 8.0, 100 m*M* NaCl. The elution profile of SYE4 was consistent with a 40 kDa protein, indicating that SYE4 is a monomeric species in solution. Final purity was confirmed by silver staining of an SDS–PAGE gel. The pure fractions were pooled and dialyzed against 50 m*M* Tris pH 8.0, 50 m*M* NaCl. The protein was subsequently concentrated to 10 mg ml^{-1} and stored at 277 K.

2.2. Dynamic light scattering

Dynamic light-scattering studies on recombinant SYE4 were performed using a Zetasizer Nano dynamic light-scattering instrument (Malvern) equipped with a 633 nm He–Ne laser and a temperature-controlled measuring chamber. Prior to all measurements, samples of purified SYE4 at 10 mg ml^{-1} in 20 m*M* Tris buffer pH 8.0 were clarified by centrifugation at 16 000*g* and filtration using 0.2 µm filters (Millipore).

2.3. Protein crystallization

Crystallization trials were set up at 295 and 277 K based on both the hanging-drop and sitting-drop vapour-diffusion methods using 300 µl reservoir solution (Crystal Screens 1 and 2; Hampton Research) and mixing equal volumes of protein solution (10 mg ml^{-1} in 50 m*M* Tris pH 8.0, 50 m*M* NaCl) and reservoir solution to form crystallization droplets (1 + 1 µl). Optimization of crystallization leads was carried out by varying a number of crystallization parameters including the concentration of precipitants and salts, the pH, temperature and protein concentration.

2.4. Preparation of crystalline SYE4–ligand complexes

Crystals of SYE4 were washed with crystal stabilization buffer (1.6 *M* sodium citrate tribasic dihydrate pH 6.3) and were subsequently incubated in the same buffer supplemented with 20 m*M* of the desired phenolic ligand [*para*-hydroxybenzaldehyde (HBA), *para*-methoxyphenol (MPH) or *para*-methylphenol (PMP)] or nitroaromatic ligand [trinitrophenol or picric acid (TNP)]. The progress of complex formation with the phenolic ligands was monitored by the change of crystal colour to lime green, indicating the establishment of charge-transfer complexes (Matthews *et al.*, 1975).

To trap a hydride–Meisenheimer (MSH) complex of a nitroaromatic ligand in crystals of SYE4, a two-step procedure was adopted. Firstly, SYE4 crystals were chemically reduced following a brief (2 min) incubation in stabilization buffer supplemented with 1 m*M* $NaBH_4$. The progress of the chemical reduction was monitored by the change of the golden yellow crystals of oxidized SYE4 to colourless. In a second step, reduced crystals were incubated overnight in crystal stabilization solution containing 20 m*M* picric acid (TNP). A very pronounced colour change from colourless to deep orange indicated that the long-lived SYE4–picrate hydride–Meisenheimer complex was likely to be formed with high occupancy (Khan *et al.*, 2002, 2004).

2.5. Crystal handling, data collection, processing and structure solution

Crystals of SYE4 were prepared for data collection under cryogenic conditions by briefly incubating them (∼1 min) in a cryoprotectant solution containing 1.6 *M* sodium citrate tribasic dihydrate pH 6.3 and 20%(*v*/*v*) glycerol. In the case of liganded SYE4 the cryoprotectant solution was supplemented with at least 20 m*M* of the corresponding ligand. The crystals were subsequently cryocooled by plunging them directly into liquid nitrogen.

X-ray diffraction data were collected at 100 K on beamlines X11 and X13 of DESY/EMBL Hamburg (Germany) and on beamline X06SA of the Swiss Light Source (Villigen, Switzerland). Data-collection strategies were chosen carefully to efficiently collect complete and redundant data to the highest resolution possible with minimal radiation damage, while accounting for spot overlaps and spot intensities beyond the dynamic range of the detectors used. For the HBA–SYE4 and MPH–SYE4 data sets several reflections were present with intensities that exceeded the dynamic range of the MAR 165 CCD detector and data collection was carried out in terms of high- and low-resolution passes. All diffraction data were processed using the *XDS* program package (Kabsch, 1993). X-ray data statistics and other parameters related to data collection are presented in Table 1.

The structure of SYE4 was determined by molecular replacement using maximum-likelihood methods implemented in the program *Phaser* (McCoy *et al.*, 2007), using a search model generated from the coordinates of *S. oneidensis* SYE1 (PDB entry 2gou; van den Hemel *et al.*, 2006), which exhibits 42% sequence identity to SYE4. In our search model nonconserved residues were replaced by alanine or glycine, while all insertions and water molecules and the FMN cofactor were omitted. Initial model building was carried out with *ARP*/*wARP* v.7.0.1 (Perrakis *et al.*, 1997), with native data truncated to 1.5 Å resolution.

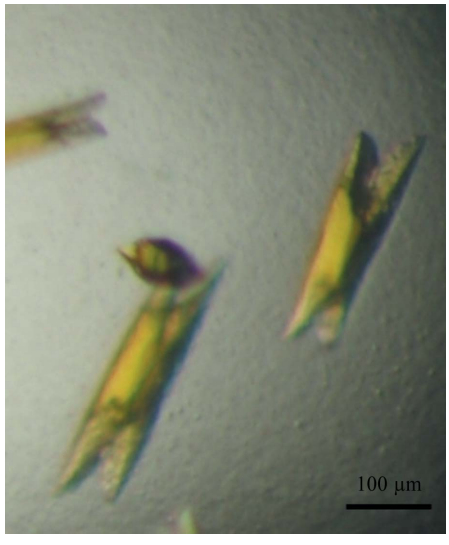

Figure 1
Crystals of SYE4. Representative crystals measuring 300 × 40 × 40 µm of the orthorhombic crystal form grown in 1.3 *M* sodium citrate tribasic dihydrate pH 6.3.

3. Results and discussion

We have established protocols for the production of recombinant SYE4, which is arguably one of the most versatile members of the OYE family, to facilitate studies of the structural enzymology of the enzyme. Typical preparations of the recombinant enzyme yielded 0.5–1 mg of >95% pure enzyme per litre of culture.

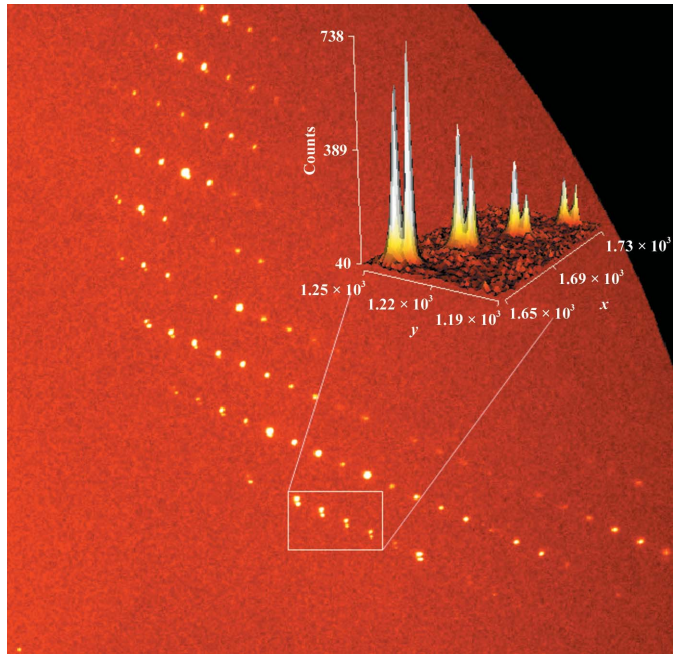

Figure 2
SYE4 low-resolution-pass diffraction pattern and spot splitting owing to pseudo-merohedral twinning. Owing to the $a \simeq b$ unit-cell parameter relation, the orthorhombic cell emulates a *P*422 tetragonal metric symmetry. The pseudo-merohedral twinning is particularly evident from the diffraction pattern; since the relation is not perfect, splitting of certain reflections in reciprocal space occurs at higher diffraction angles. The inset shows a three-dimensional representation of a selected part of the detector surface. The split reflection intensities are nonetheless summed in the same integration box by *XDS*. This low-resolution pass image was collected using a MAR CCD 165 detector from a crystal frozen at 100 K on DESY/EMBL beamline X11. The nominal resolution at the edge of the detector is 2.42 Å; the large crystal-to-detector distance allowed the spot splitting to be visualized. Figures were prepared with the *PROTEUM*2 suite (Bruker AXS Inc., Madison, Wisconsin, USA).

Crystallization trials using monodisperse purified recombinant SYE4 led to the growth of rectangular golden yellow SYE4 crystals on a background of precipitate in condition 28 (1.6 *M* sodium citrate tribasic dihydrate pH 6.5) of Crystal Screen 2 (Hampton Research) within one month at room temperature. Further exploration of this lead condition by varying a number of crystallization parameters led reproducibly to diffraction-quality crystals typically measuring 0.040 × 0.040 × 0.300 mm within a week in droplets containing 1.3–1.4 *M* sodium citrate tribasic dihydrate pH 6.3 (Fig. 1). Native crystals of SYE4 diffracted to a nominal resolution of 1.00 Å using highly brilliant synchrotron radiation. The crystals belonged to the orthorhombic space group $P2_12_12_1$, with unit-cell parameters a = 52.24, b = 54.85, c = 103.60 Å, and contained one molecule per asymmetric unit, with a V_M value of 1.90 Å^3 Da^{-1}. The diffraction quality of the SYE4 crystals is exceptional for a 40 kDa protein and has set the stage for dissection of the structure–function properties of the enzyme at atomic resolution. In the case of flavoenzyme oxidoreductases, crystallographic analysis at atomic resolution has provided important mechanistic details, especially with respect to the enzyme-induced distortion of chemical group geometries and the importance of stereoelectronic effects in flavin-mediated catalysis (Berkholz *et al.*, 2008). Indeed, a query in the Protein Data Bank (http://www.rcsb.org) returned a mere 25 unique entries determined at true atomic resolution (0.9–1.1 Å resolution) for structures larger than 40 kDa per chain. In a more general context, we expect that our structural studies of SYE4 at atomic resolution will contribute important data towards the annotation of main-chain conformational space and peptide geometry in proteins (Berkholz *et al.*, 2009).

While native SYE4 crystals lose their exceptional diffraction capacity somewhat when incubated with a variety of phenolic ligands, they still yield high-quality data to near-atomic resolution (Table 1). One of the most elusive ligand complexes for OYE-family proteins has been the hydride–Meisenheimer complex, resulting from the two-electron reduction of the explosive chemical trinitrophenol (TNP), a derivative of trinitrotoluene (TNT). Indeed, owing to the ability of OYE homologues to engage in charge-transfer interactions with a variety of often hazardous phenolic compounds and derivatives thereof, OYEs have emerged as promising agents in bioremediation processes (Williams *et al.*, 2004; French *et al.*, 1999; Hannink *et al.*, 2001; Khan *et al.*, 2004). To reveal the structural basis of TNP inac-

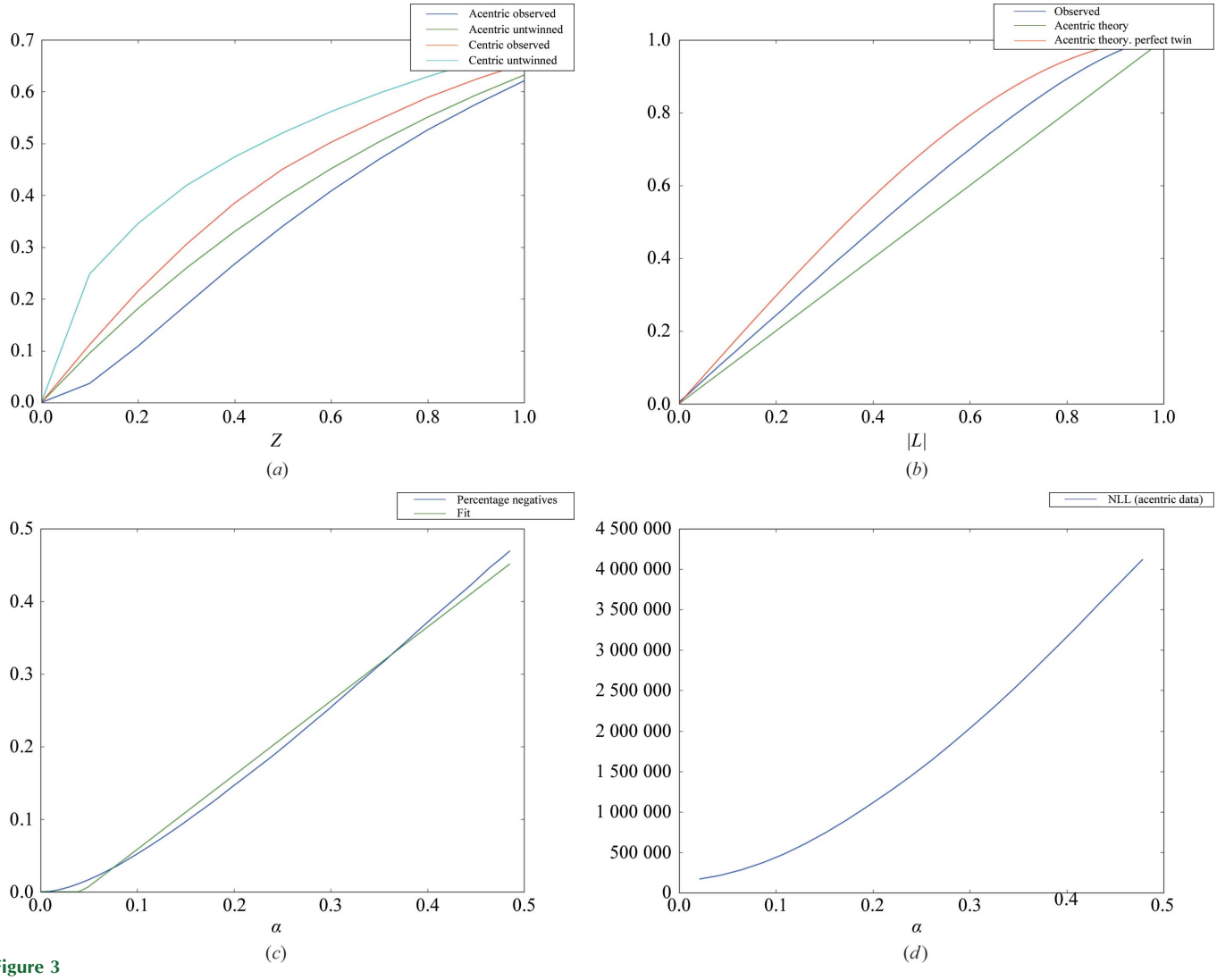

Figure 3
Diagnostic plots showing that SYE4 is pseudo-merohedrally twinned. Multiple lines of evidence suggest the existence of twinning in SYE4 crystals. (*a*) The sigmoidal shape of the cumulative intensity distribution. (*b*) The *L*-test, which compares reflections close in reciprocal space. (*c*) The Britton test suggests a twin fraction of 0.045, which is consistent with (*d*) the maximum-likelihood (ML) estimation and refined α (0.030). Figures were prepared with the graphical user interface of *phenix.xtriage* as implemented in the *PHENIX* suite of programs (Adams *et al.*, 2002).

tivation by SYE4, we established a novel approach that allowed us to first reduce SYE4 crystals *in situ* using $NaBH_4$, followed by complex formation with TNP to invoke the two-electron reduction. The use of $NaBH_4$ arose as an alternative approach to chemically reduce SYE4 crystals when attempts to do so *via* conventional treatment with NAD(P)H, the physiological reducing cofactor for OYE-family members, failed. We can now attribute the inability of NAD(P)H to reduce SYE4 crystals to the very dense crystal lattice packing of SYE4 (solvent content of ∼30%) which renders the cofactor-binding site virtually inaccessible to a relatively large ligand such as NAD(P)H. Diffusion and thus soaking of the smaller phenolic and nitro-aromatic compounds to high occupancy were not affected by the dense crystal packing, as verified *via* preliminary difference density maps calculated using Fourier coefficients $F_{\rm obs,soak} - F_{\rm obs,native}$ and calculated phases from the high-resolution native structure.

Our analysis of low-resolution-pass diffraction images from SYE4 crystals (native and charge-transfer complexes with phenolic ligands) consistently revealed split reflections at higher scattering angles (Fig. 2). We therefore wondered whether this was a consequence of the presence of a non-merohedral twin relation, *i.e.* a randomly oriented second crystal domain. The 'interdigitating' growth pattern of the crystals also gave indications supporting this hypothesis. Diffraction data collected as MAR CCD frames were read into the *PROTEUM*2 suite (Bruker AXS Inc., Madison, Wisconsin, USA) of crystallographic software and were subsequently analyzed using *CELL_NOW* (Sheldrick, 2004) and *SAINT* (Bruker AXS Inc., Madison, Wisconsin, USA). During integration, the reflection profile became elongated in one direction (which was likely to be caused by the spot splitting), but integration as a non-merohedral twin with two domains was not possible (results not shown). Therefore, we shifted our attention to the possibility that the spot splitting might arise from an imperfect pseudo-merohedral twin relation.

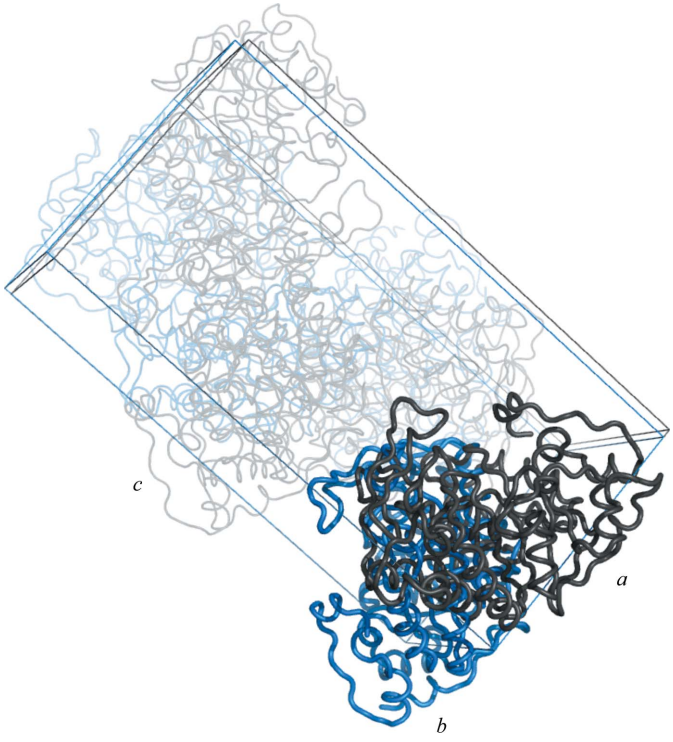

Figure 4
C^{α}-atom traces and packing of native SYE4 (black) and MSH–SYE4 (blue) in their respective primitive orthorhombic unit cells. Note that MSH–SYE4 has a rearranged unit cell and the protein model is rotated by a 180° rotation around an axis approximately parallel to the unit-cell *c* axis when compared with the model for native SYE4. This figure was prepared with *PyMOL* (DeLano, 2002).

The orthorhombic space group $P2_12_12_1$ does not allow twinning by merohedry to occur. However, in the case of fortuitous unit-cell parameters, pseudo-merohedral twinning is a possibility. As can be deduced from the dimensions of the SYE4 lattice, the unit cell exhibits approximate $a \simeq b$ and $a \simeq c/2$ relations. The condition $a \simeq b$ is a pseudo-merohedral relation whereby the orthorhombic cell emulates a *P*422 metric symmetry under the twin operator $k, h, -l$. The condition $a \simeq c/2$ is a potential non-merohedral twin in which all $l = 2n$ reflections would be affected. This latter relation is seen quite frequently in small-molecule crystallography. Converting our data to an HKLF 5 format in which the $l = 2n$ reflections were flagged gave no evidence to this hypothesis, with the *SHELXL* batch scale factor (BASF) refining to unrealistically low values (results not shown). Pseudo-merohedral twinning was further investigated systematically using the programs *phenix.xtriage* (Adams *et al.*, 2002) and *SFCHECK* (Vaguine *et al.*, 1999) and was shown to occur in all data sets except for the hydride–Meisenheimer (MSH–SYE4) data set (Fig. 3). The estimated twin fraction varied between the data sets from 2 to 5%. Interestingly, the SYE4 hydride–Meisenheimer complex has a slightly rearranged unit cell such that the approximate $a \simeq b$ relation is no longer valid, resulting in the disappearance of the pseudo-merohedral twin law (Table 1).

The structure of SYE4 was determined by maximum-likelihood molecular replacement implemented in *Phaser* (McCoy *et al.*, 2007) using a conservative search model based on the structure of SYE1 (van den Hemel *et al.*, 2006). The correctness of the structure solution was initially assessed with the help of difference electron-density maps calculated with Fourier coefficients $2F_{\rm o} - F_{\rm c,MR}$, $\alpha_{\rm MR}$ and $F_{\rm o} - F_{\rm c,MR}$, $\alpha_{\rm MR}$ after refinement of the placed search model by rigid-body refinement. This initial set of phases was subsequently input into *ARP*/*wARP* v.7.0.1 (Perrakis *et al.*, 1997), which allowed reconstruction of 95% of the model (Fig. 4). All phenolic complexes of SYE4 are essentially isomorphous to native SYE4 except for the hydride–Meisenheimer complex, which exhibits a dramatic 180° rotation around an axis roughly parallel to the unit-cell *c* axis (Fig. 4).

Refinement of the ultrahigh-resolution native structure and the *p*-HBA (*para*-hydroxybenzaldehyde) soaked structure (HBA–SYE4) is under way using the *SHELXL* refinement program (Sheldrick, 2008), while all other structures are being refined with the *PHENIX* suite (Adams *et al.*, 2002). Here, we provide details of our refinement approach for the native SYE4 to 1.1 Å resolution, as we feel that it might be of general interest given the growing application of the program *SHELXL* in macromolecular structure refinement at atomic resolution. Our protocol employs conjugate-gradient least-squares refinement and blocked full-matrix least-squares inversion for the estimation of the r.m.s. deviations of bonds and angles. Individual atoms are refined anisotropically using the suggested SIMU and DELU restraints, while no such restraints were applied for the FMN cofactor. The default value for the DELU standard deviation was used and the standard deviation of SIMU was altered to 0.025, *i.e.* the restraint was tightened, resulting in a more symmetric distribution of anisotropy with a mean anisotropy of 0.488 and similar U_{ij} values between neighbouring atoms. The ISOR restraint is only applied to solvent atoms. In further steps of refinement, 'riding' H atoms were added to the model, the resolution was extended and the weighting scheme adjusted as suggested by *SHELXL* to give more weight to the X-ray terms. During the course of refinement we noted that good convergence and stability of least-squares refinement were crucially dependent on inclusion of the twin operator $(k, h, -l)$, despite the low twin fraction. This was further supported by the consistently

improving goodness of fit (GooF) with respect to the experimental data (typically a drop of 0.05 units) and the concomitant drop in $R/R_{\rm free}$ (about 1%). The twin fractions refined by *SHELXL* are in good agreement with those predicted by the diagnostic tests (Fig. 3).

We gratefully acknowledge beam-time allocation and technical support provided at beamlines X11 and X13 of DESY/EMBL (Hamburg, Germany) and beamline X06SA of the SLS (Villigen, Switzerland). JE is a research fellow of the Research Foundation Flanders (FWO), Belgium. This work was supported by start-up research funds from Ghent University to SNS.

References

Abramovitz, A. S. & Massey, V. (1976). *J. Biol. Chem.* **251**, 5327–5336.
Adams, P. D., Grosse-Kunstleve, R. W., Hung, L.-W., Ioerger, T. R., McCoy, A. J., Moriarty, N. W., Read, R. J., Sacchettini, J. C., Sauter, N. K. & Terwilliger, T. C. (2002). *Acta Cryst.* D**58**, 1948–1954.
Berkholz, D. S., Faber, H. R., Savvides, S. N. & Karplus, P. A. (2008). *J. Mol. Biol.* **382**, 371–384.
Berkholz, D. S., Shapovalov, M. V., Dunbrack, R. L. Jr & Karplus, P. A. (2009). *Structure*, **17**, 1316–1325.
Biesgen, C. & Weiler, E. W. (1999). *Planta*, **208**, 155–165.
Blehert, D. S., Fox, B. G. & Chambliss, G. H. (1999). *J. Bacteriol.* **181**, 6254–6263.
Brigé, A., van den Hemel, D., Carpentier, W., De Smet, L. & Van Beeumen, J. J. (2006). *Biochem. J.* **394**, 335–344.
DeLano, W. L. (2002). *The PyMOL Molecular Viewer.* http://www.pymol.org.
Fitzpatrick, T. B., Amrhein, N. & Macheroux, P. (2003). *J. Biol. Chem.* **278**, 19891–19897.
French, C. E. & Bruce, N. C. (1994). *Biochem. J.* **301**, 97–103.
French, C. E. & Bruce, N. C. (1995). *Biochem. J.* **312**, 671–678.
French, C. E., Nicklin, S. & Bruce, N. C. (1996). *J. Bacteriol.* **178**, 6623–6627.
French, C. E., Rosser, S. J., Davies, G. J., Nicklin, S. & Bruce, N. C. (1999). *Nature Biotechnol.* **17**, 491–494.
Hannink, N., Rosser, S. J., French, C. E., Basran, A., Murray, J. A., Nicklin, S. & Bruce, N. C. (2001). *Nature Biotechnol.* **19**, 1168–1172.
Hemel, D. van den, Brigé, A., Savvides, S. N. & Van Beeumen, J. (2006). *J. Biol. Chem.* **281**, 28152–28161.
Kabsch, W. (1993). *J. Appl. Cryst.* **26**, 795–800.
Khan, H., Barna, T., Harris, R. J., Bruce, N. C., Barsukov, I., Munro, A. W., Moody, P. C. & Scrutton, N. S. (2004). *J. Biol. Chem.* **279**, 30563–30572.
Khan, H., Harris, R. J., Barna, T., Craig, D. H., Bruce, N. C., Munro, A. W., Moody, P. C. & Scrutton, N. S. (2002). *J. Biol. Chem.* **277**, 21906–21912.
Kubata, B. K., Kabututu, Z., Nozaki, T., Munday, C. J., Fukuzumi, S., Ohkubo, K., Lazarus, M., Maruyama, T., Martin, S. K., Duszenko, M. & Urade, Y. (2002). *J. Exp. Med.* **196**, 1241–1251.
Massey, V. (2000). *Biochem. Soc. Trans.* **28**, 283–296.
Matthews, R. G. & Massey, V. (1969). *J. Biol. Chem.* **244**, 1779–1786.
Matthews, R. G., Massey, V. & Sweeley, C. C. (1975). *J. Biol. Chem.* **250**, 9294–9298.
McCoy, A. J., Grosse-Kunstleve, R. W., Adams, P. D., Winn, M. D., Storoni, L. C. & Read, R. J. (2007). *J. Appl. Cryst.* **40**, 658–674.
Perrakis, A., Sixma, T. K., Wilson, K. S. & Lamzin, V. S. (1997). *Acta Cryst.* D**53**, 448–455.
Schaller, F., Biesgen, C., Mussig, C., Altmann, T. & Weiler, E. W. (2000). *Planta*, **210**, 979–984.
Schaller, F. & Weiler, E. W. (1997). *J. Biol. Chem.* **272**, 28066–28072.
Sheldrick, G. M. (2004). *CELL_NOW.* University of Göttingen, Germany.
Sheldrick, G. M. (2008). *Acta Cryst.* A**64**, 112–122.
Strassner, J., Furholz, A., Macheroux, P., Amrhein, N. & Schaller, A. (1999). *J. Biol. Chem.* **274**, 35067–35073.
Vaguine, A. A., Richelle, J. & Wodak, S. J. (1999). *Acta Cryst.* D**55**, 191–205.
Williams, R. E. & Bruce, N. C. (2002). *Microbiology*, **148**, 1607–1614.
Williams, R. E., Rathbone, D. A., Scrutton, N. S. & Bruce, N. C. (2004). *Appl. Environ. Microbiol.* **70**, 3566–3574.